



Cite this: *Phys. Chem. Chem. Phys.*,  
2015, 17, 8499

## Exploring volume, compressibility and hydration changes of folded proteins upon compression

Vladimir P. Voloshin,<sup>a</sup> Nikolai N. Medvedev,<sup>ab</sup> Nikolai Smolin,<sup>c</sup> Alfons Geiger<sup>d</sup> and Roland Winter<sup>\*d</sup>

Understanding the physical basis of the structure, stability and function of proteins in solution, including extreme environmental conditions, requires knowledge of their temperature and pressure dependent volumetric properties. One physical–chemical property of proteins that is still little understood is their partial molar volume and its dependence on temperature and pressure. We used molecular dynamics simulations of aqueous solutions of a typical monomeric folded protein, staphylococcal nuclease (SNase), to study and analyze the pressure dependence of the apparent volume,  $V_{app}$ , and its components by the Voronoi–Delaunay method. We show that the strong decrease of  $V_{app}$  with pressure ( $\beta_T = 0.95 \times 10^{-5} \text{ bar}^{-1}$ , in very good agreement with the experimental value) is essentially due to the compression of the molecular volume,  $V_M$ , ultimately, of its internal voids,  $V_M^{empty}$ . Changes of the intrinsic volume (defined as the Voronoi volume of the molecule), the contribution of the solvent to the apparent volume, and of the contribution of the boundary voids between the protein and the solvent have also been studied and quantified in detail. The pressure dependences of the volumetric characteristics obtained are compared with the temperature dependent behavior of these quantities and with corresponding results for a natively unfolded polypeptide.

Received 15th January 2015,  
Accepted 6th February 2015

DOI: 10.1039/c5cp00251f

www.rsc.org/pccp

### Introduction

The physical–chemical properties of proteins, which include their functional and unique three dimensional structure, their stability and conformational dynamics, are coupled to varying degrees and result from the specific amino acid sequence of which they are composed.<sup>1–3</sup> Understanding the relationship between the amino acid sequence and these properties has fascinated protein chemists and physicists for decades now. One physical–chemical property of proteins that has received comparably little attention over the years is its partial molar volume and its dependence on temperature and pressure. Also the factors contributing to the volumetric properties of proteins have long eluded understanding. This holds in particular true for pressure dependent volumetric properties despite the fact that it has already been known by Nobel laureate P. W. Bridgman in 1914 that the application of pressure can lead to the unfolding of proteins.<sup>4</sup> Since then, many studies have been carried out employing pressure to study protein dissociation and unfolding.<sup>5–20</sup> According

to Le Châtelier's principle, the effect of pressure necessarily arises because the volume of the dissociated or unfolded state is smaller than that of the associated or folded state. Understanding of both, the temperature and pressure dependent volumetric changes are prerequisite for understanding the physical basis of protein structure, stability and function,<sup>20–25</sup> including the influence of extreme environmental conditions such as those encountered in the deep sea where pressures up to the kbar level are reached. In particular, since the 1970's it has been known<sup>6–9</sup> that appropriate modeling of experimental  $p$ - $T$  phase diagrams for protein folding requires, in addition to the difference in enthalpy, entropy and heat capacity between the unfolded (U) and folded (F) state, knowledge of the difference in their volumes,  $\Delta V_{U,F}$ , but also in their thermal expansivity,  $\Delta \alpha_{U,F}$ , and isothermal compressibility,  $\Delta \beta_{T,U,F}$ . At low temperatures,  $\Delta V_{U,F}$  has been found to be generally negative (*i.e.*, the application of pressure leads to unfolding under these conditions), but decreases in absolute value approaching zero as temperature increases, and can even become positive at high temperatures,<sup>6,8,10–15,23–26</sup> indicating that the thermal expansivity of the unfolded state is larger than that of the folded state. The change in the partial molar volume (or the apparent volume,  $V_{app}$ , *i.e.* the partial molar volume at infinite dilution) upon pressure-induced unfolding of a protein,  $V_{app,U} - V_{app,F}$ , is generally thought to be due to the opening and subsequent filling of void volume and the increase in hydrophilic hydration of charged and polar polypeptide groups upon exposure to the bulk solvent. The method of dissecting this volume change,

<sup>a</sup> Institute of Chemical Kinetics and Combustion, SB RAS, 630090 Novosibirsk, Russia

<sup>b</sup> Novosibirsk State University, 630090 Novosibirsk, Russia

<sup>c</sup> Department of Cell and Molecular Physiology, Stritch School of Medicine, Loyola University Chicago, Maywood, Illinois 60153, USA

<sup>d</sup> Physikalische Chemie, Fakultät für Chemie und Chemische Biologie, Technische Universität Dortmund, Otto-Hahn-Strasse 6, 44221 Dortmund, Germany. E-mail: roland.winter@tu-dortmund.de; Tel: +49 231 755 3900

and hence  $V_{\text{app}}$ , into its different contributions and their magnitudes are still a matter of debate, however.<sup>5,21–27</sup>

In this study, we analysed the contributions to the measured volumetric properties of a well characterized monomeric folded protein, staphylococcal nuclease (SNase), and its pressure dependence, *i.e.* the isothermal compressibility, using results from molecular dynamics (MD) simulations and the dissection of the MD model into Voronoi and Delaunay shells. The theoretical data obtained are then compared with experimental data as determined by densitometry.<sup>15</sup> The volumetric properties are resolved into their various structural, interfacial and hydrational contributions, aiming to help quantitatively understand the volumetric properties of proteins upon compression, which is prerequisite for understanding pressure-induced conformational changes of proteins and of biomolecules in general.

## Methods

### Molecular dynamics simulation setup

We used MD simulations to study the SNase molecule in aqueous solution for five different pressures (from 1 to 2000 bar) at constant temperature of 300 K. The simulations were carried out using the simulation package GROMACS<sup>28,29</sup> with the OPLS force field<sup>30</sup> for the protein and the SPC/E water model.<sup>31</sup> An initial energy minimization of the SNase structure was performed using the steepest descent method for 1000 steps, after that the protein was solvated in a rectangular water box with a minimum of 15 Å from the surface of the protein to a face of the model box. Thus, the SNase molecule was surrounded by 16 838 water molecules. The Particle Mesh Ewald (PME) method<sup>32,33</sup> was used to calculate the electrostatic interactions, and a cut-off of 9 Å was used for the short-range Van der Waals interactions. The MD simulations were carried out with an integration time step of 2 fs. After 1 ns equilibration, production simulations were performed in the *NPT* ensemble using the Nose–Hoover thermostat<sup>34,35</sup> and a Parrinello–Rahman barostat<sup>36,37</sup> with relaxation times of 2.5 ps and 1.0 ps, respectively. The production run was carried out for 50 ns for each pressure. 5000 equally spaced snapshots of the production run were used for averaging the volumetric properties of the protein.

### Voronoi–Delaunay method

The Voronoi–Delaunay method has been widely used in biomolecular science over the years<sup>38–44</sup> and has been described in detail elsewhere.<sup>45–47</sup> Recently, we started applying this method also to calculations of volumetric properties of biomolecular systems. In particular, the method was used to reveal volumetric properties of polypeptides, amphiphilic molecules, and of methane.<sup>48–53</sup>

The first step is the calculation of the Voronoi–Delaunay tessellation for given configurations of the molecular dynamics model of the solution. The water molecules are considered here as single spheres. The atoms of the dissolved molecule are considered as overlapping spheres with diameters equal to the values of their Lennard-Jones parameters,  $\sigma$ , used in the molecular dynamics simulation. For the volumetric analysis

we need to take into account the size of the atoms. Thus, instead of the classical Voronoi–Delaunay tessellation (which is defined for discrete points) we have to use the S-tessellation (additively weighted)<sup>42,45,54</sup> or radical (power) tessellation<sup>55,56</sup> method, which take into account atomic radii. As in our last works, we used the radical tessellation approach, because an efficient calculation of the empty volume inside systems of overlapping spheres has been implemented only for this type of the tessellation.<sup>57</sup> The S-tessellation was used in ref. 48 and it was found that the physical conclusions derived do not depend on which one of these two tessellations was used. The calculation of the Voronoi–Delaunay tessellation is a straightforward task. In this work, we used our algorithms, but programs for calculation of radical tessellations are available also in standard geometry libraries.

The second step is the decomposition of the tessellation into Voronoi and Delaunay shells around the solute molecule.<sup>38,48,50</sup> To this end, we can define the boundary Voronoi shell of the solute molecule, which consists of those Voronoi cells of the protein atoms that are adjacent to at least one molecule of the solvent. With this information in hand, one can select all subsequent Voronoi shells, both going outside (to the solvent) and inside the solute molecule (if it is large enough).<sup>50</sup> The decomposition into Voronoi shells can then be used for determining Delaunay shells. A Delaunay shell is defined as the set of Delaunay simplexes with vertices (atoms) belonging to two neighboring Voronoi shells. Fig. 1 (thick dotted lines) illustrates the boundary Delaunay shell. As the Delaunay simplexes are centered on the void space between atoms, this construction allows the definition of the empty space at the boundary between protein and solvent (denoted “boundary voids” in the following, green area in Fig. 1).

Volumetric investigations require calculation of the empty or occupied volume of Voronoi cells and Delaunay simplexes. This is not a simple task for an ensemble of overlapping spheres, such as encountered for molecular systems. An efficient solution to this problem has been found recently with the help of a special geometrical construction, called Voronoi–Delaunay subsimplex.<sup>58</sup> Using this approach, we can determine the empty volume of the entire Voronoi and Delaunay shells as well as their intersections.<sup>57</sup>

### Volumetric characteristics

The apparent volume of a solute in solution from a molecular dynamics model can be calculated, by definition, as the difference between the volume of the model box containing the solution, and the volume of the model box containing the same amount of the pure solvent:<sup>53,59,60</sup>

$$V_{\text{app}} = V_{\text{box}}^{\text{solution}} - V_{\text{box}}^{\text{solvent}} \quad (1)$$

As in this case  $V_{\text{app}}$  would be determined as a small difference between two large numbers, it is preferable to determine  $V_{\text{app}}$  as the asymptotic value of

$$V_{\text{app}}(R) = V(R) - N(R)/\rho_0, \quad (2)$$

where  $V(R)$  is the volume including both the solute and its hydration shell.<sup>52,53,61–63</sup> The parameter  $R$  characterizes the size of this region.  $N(R)$  is the number of the solvent molecules, whose centers are located inside the selected volume, and  $\rho_0$  is

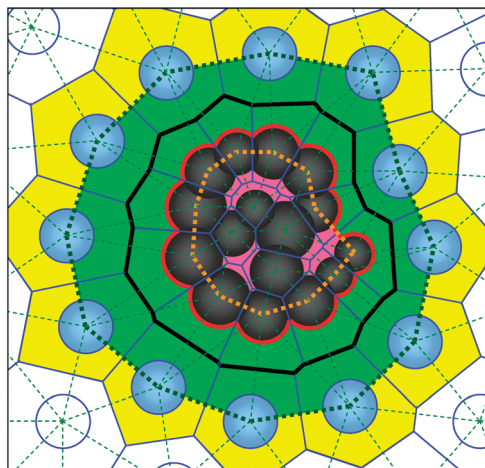


**Fig. 1** 2D illustration of the volumetric characteristics of the Voronoi–Delaunay method. Dark disks designate the solute molecule, blue and empty disks in the surroundings represent water molecules. The molecular volume,  $V_M$  is outlined by a thick red line. It contains the van der Waals volume of the molecule  $V_M^{\text{vdW}}$  (union of dark discs) and the internal void contribution,  $V_M^{\text{empty}}$  (colored in pink). The surface of the molecular volume consists of parts of atomic surfaces and parts of Delaunay simplex faces. The Voronoi volume of the molecule,  $V_{\text{Vor}}$ , is bounded by a thick black line. It contains the molecular volume  $V_M$  and part of the boundary voids,  $V_B^M$  (dark green). The total boundary empty volume,  $V_B$ , is shown in green (dark and light). It includes all voids inside the boundary Delaunay shell, shown by thick dotted lines (green and pink). The boundary empty volume is divided by the Voronoi surface of the solute into a part assigned to the solute molecule ( $V_B^M$ ) and a part belonging to the solvent,  $V_B^S$  (light-green), which is also the inner part of the empty volume of the first Voronoi shell. The outer part of the first Voronoi shell is shown in yellow. Voronoi cells and Delaunay simplexes of the solution are shown by thin solid and dotted lines, respectively.

the number density of pure (bulk) water. This formula, which is a variant of the Kirkwood–Buff integral, can generally be used, but becomes more preferable if the solute molecule perturbs the solvent on short distances only, like it was shown for proteins.<sup>48</sup> Recently, we proposed to calculate  $V(R)$  as the sum of the Voronoi cell volumes of all atoms with centers inside a defined  $R$ -surface. This method turned out to be very efficient, and we denoted it *combined method* in our works.<sup>48,52,53</sup>

The apparent volume of the solute molecule in solution can be divided into the *intrinsic volume*, and the *contribution of the solvent*,  $\Delta V$ :

$$V_{\text{app}} = V_{\text{int}} + \Delta V. \quad (3)$$

Here, the intrinsic volume is assigned to the *Voronoi volume* of the molecule in solution,  $V_{\text{Vor}}$ .<sup>40,63</sup>

$$V_{\text{app}} = V_{\text{Vor}} + \Delta V. \quad (4)$$

In Fig. 1, the Voronoi volume of the solute is marked by thick black lines. From the Voronoi tessellation of the computer model of a solution,  $V_{\text{Vor}}$  is readily obtained as the sum of the volumes of the Voronoi cells of all solute atoms. With the knowledge of  $V_{\text{app}}$  and  $V_{\text{Vor}}$  we can then determine the solvent contribution,

$$\Delta V = V_{\text{app}} - V_{\text{Vor}}. \quad (5)$$

This is a general definition of the solvent contribution and includes all possible contributions of the solvent to

the apparent volume apart from the volume assigned to the solute molecule.

The Voronoi volume of the solute molecules can be dissected into the molecular volume,  $V_M$ , and the part of boundary empty space,  $V_B^M$ , that is assigned to the solute,

$$V_{\text{Vor}} = V_M + V_B^M. \quad (6)$$

Thus, the Voronoi volume of the molecule can be interpreted as the volume of a cavity in solution where the solute molecule has been placed.

The molecular volume,  $V_M$ , is depicted in Fig. 1 by a thick red line. It contains the van der Waals volume of the molecule,  $V_M^{\text{vdW}}$ , and the internal void volume,  $V_M^{\text{empty}}$ :

$$V_M = V_M^{\text{vdW}} + V_M^{\text{empty}}. \quad (7)$$

In our Voronoi–Delaunay method, we can explicitly determine all these regions (Fig. 1), and calculate their volumes.<sup>57</sup> Please recall that the value  $V_M^{\text{vdW}}$  is defined as the volume of the entirety of spheres (atoms of the molecule), and can be easily calculated as the sum of the occupied volumes of their Voronoi cells.<sup>57,64</sup> The value of  $V_M^{\text{empty}}$  is the empty volume of the Delaunay simplexes, which represent the inner voids of the dissolved molecule (*i.e.* the Delaunay simplexes having vertices that lie only on the atoms of the solute molecule).<sup>50</sup> Some volumetric characteristics can be calculated in different ways. For example,  $V_B^M$  can be calculated from eqn (6) as remainder of  $V_{\text{Vor}}$  and  $V_M$ , or directly, as the empty volume of the intersection of the boundary Voronoi and Delaunay shells.<sup>57</sup>

In addition to eqn (5), the contribution  $\Delta V$  can also be defined directly as the difference between the volume of the hydration shell surrounding the solute and the volume of the same amount of water molecules ( $N_{\text{hyd}}$ ) in the bulk:<sup>60</sup>

$$\Delta V = V_{\text{hyd}} - N_{\text{hyd}}/\rho_0. \quad (8)$$

Here,  $\rho_0$  is the density of bulk water at the same temperature and pressure. However, in this approach, one has to define explicitly the borders of the hydration shell. It turns out that the result is very sensitive to the definition of this shell and may lead to erroneous results as it was discussed before.<sup>48</sup> However, in our Voronoi–Delaunay approach, where the border is well defined as the Voronoi surface of the solute molecule, formulas (5) and (8) are equivalent.<sup>53</sup>

Using eqn (6) and (7) we can write a more detailed decomposition of the apparent volume, instead of eqn (4):

$$V_{\text{app}} = V_M^{\text{vdW}} + V_M^{\text{empty}} + V_B^M + \Delta V, \quad (9)$$

where the  $\Delta V$  value can be calculated by eqn (5), or independently by eqn (8).

Using the boundary Delaunay shell, we can calculate the boundary voids,  $V_B$ , between the solute and solvent (green area (dark and light) in Fig. 1). The border of the Voronoi volume of the solute molecule divides this volume into two parts:

$$V_B = V_B^M + V_B^S. \quad (10)$$

$V_B^M$  is the empty space closest to the solute molecule (dark green in Fig. 1). It belongs to the solute, not to the surrounding

water molecules. In contrast, the second part (light green in Fig. 1) is part of the solvent.

## Results and discussion

### The Voronoi–Delaunay method for dissecting the apparent volume of a protein

Fig. 2 shows the pressure dependence of the apparent volume,  $V_{\text{app}}$ , of SNase at ambient temperature and its components,  $V_{\text{Vor}}$  and  $\Delta V$ , as defined in eqn (4). The compressibility of  $V_{\text{app}}$  is positive (see also Table 1), and its value is in very good agreement with the experimental value  $\beta_T = 1.1 \pm 0.2 \times 10^{-5} \text{ bar}^{-1}$  at 298 K as obtained from direct densitometric measurements.<sup>15</sup> What we can also see is that the observed decrease of the apparent volume with pressure is the result of the competition between the decrease of the intrinsic (Voronoi) volume of the solute ( $V_{\text{Vor}}$ ) and the increase of the contribution of the solvent ( $\Delta V$ ).

Fig. 3 reveals the strong decrease of  $V_{\text{Vor}}$  upon pressurization. Pressure reduces both, the molecular volume  $V_{\text{M}}$  and the boundary empty volume assigned to the molecule,  $V_{\text{B}}^{\text{M}}$ .

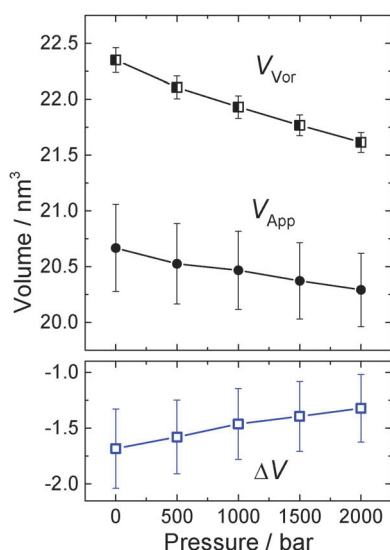


Fig. 2 The apparent volume,  $V_{\text{app}}$ , and its components,  $V_{\text{Vor}}$  and  $\Delta V$ , of SNase as a function of pressure at  $T = 300 \text{ K}$ . Vertical lines show the mean square displacement of the calculated values (over 5000 independent configurations). Fluctuations of the apparent volume are mainly determined by the solvent.

Table 1 Coefficients of isothermal compressibility of SNase,  $\beta_T = -(\text{d}V/\text{d}p)/V_{\text{app}}/\text{bar}^{-1}$ , for  $V_{\text{app}}$  and its various components ( $T = 300 \text{ K}$ )

$-(\text{d}V_{\text{app}}/\text{d}p)/V_{\text{app}}$	$0.95 \times 10^{-5}$
$-(\text{d}V_{\text{M}}/\text{d}p)/V_{\text{app}}$	$1.00 \times 10^{-5}$
$-(\text{d}\Delta V/\text{d}p)/V_{\text{app}}$	$-0.88 \times 10^{-5}$
$-(\text{d}V_{\text{M}}^{\text{dW}}/\text{d}p)/V_{\text{app}}$	$0.05 \times 10^{-5}$
$-(\text{d}V_{\text{M}}^{\text{empty}}/\text{d}p)/V_{\text{app}}$	$0.95 \times 10^{-5}$
$-(\text{d}V_{\text{Vor}}/\text{d}p)/V_{\text{app}}$	$1.83 \times 10^{-5}$
$-(\text{d}V_{\text{B}}^{\text{M}}/\text{d}p)/V_{\text{app}}$	$0.83 \times 10^{-5}$
$-(\text{d}V_{\text{B}}/\text{d}p)/V_{\text{app}}$	$1.76 \times 10^{-5}$
$-(\text{d}V_{\text{B}}^{\text{S}}/\text{d}p)/V_{\text{app}}$	$0.93 \times 10^{-5}$
$-(\text{d}V_{\text{B}}^{\text{S,bulk}}/\text{d}p)/V_{\text{app}}$	$1.81 \times 10^{-5}$

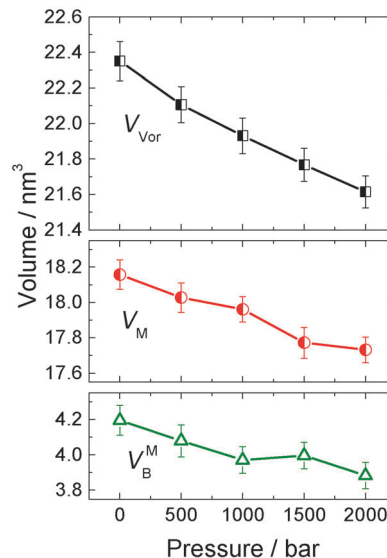


Fig. 3 Pressure dependence of the components of the intrinsic (Voronoi) volume of SNase at  $T = 300 \text{ K}$  ( $V_{\text{Vor}} = V_{\text{M}} + V_{\text{B}}^{\text{M}}$ ).

Please note that the decrease of  $V_{\text{M}}$  is provided solely by the internal voids of the solute, *i.e.*  $V_{\text{M}}^{\text{empty}}$  because the van der Waals volume is not sensitive to pressure (Fig. 4a).<sup>51</sup> The same is true for the temperature dependence (Fig. 4b): the expansion of  $V_{\text{M}}$  is completely determined by the expansion of the empty space,  $V_{\text{M}}^{\text{empty}}$ .

Fig. 5a reveals a general shrinking of the void volume at the solute/solvent interface upon compression. The total void volume,  $V_{\text{B}}$ , decreases by  $\sim 4\%/k\text{bar}$  and its components  $V_{\text{B}}^{\text{M}}$  and  $V_{\text{B}}^{\text{S}}$  exhibit a similar pressure dependence. A parallel behavior of  $V_{\text{B}}^{\text{M}}$  and  $V_{\text{B}}^{\text{S}}$  was also found for the temperature dependence (Fig. 5b).<sup>49</sup>

Comparing the pressure and temperature dependence of  $V_{\text{M}}^{\text{empty}}$  (Fig. 4), we note that a change in temperature by 200 K and a pressure change of 2000 bar lead to similar changes of the value of  $V_{\text{M}}^{\text{empty}}$  ( $\approx 0.5 \pm 0.1 \text{ nm}^3$ ). On the other hand, a comparison with the changes of the boundary volume of the solute over the same temperature and pressure range reveals that the boundary voids,  $V_{\text{B}}$ , are relatively more sensitive to temperature than to pressure (with absolute value changes of 3.1 and 0.6  $\text{nm}^3$ , respectively). The temperature-induced change of the volume of the boundary voids is 5 times larger than the corresponding pressure-induced change.

Thus, Fig. 3 to 5 indicate that the pressure dependence of the Voronoi volume,  $V_{\text{Vor}}$ , of the solute is caused both by a pronounced decrease of the molecular volume (due to a decrease of the internal void volume), and by the densification of the protein/solvent interface upon compression. A similar situation, but with opposite sign, is observed for the temperature dependence of the Voronoi volume (see ref. 49 and Fig. 4 and 5). It is caused both by a pronounced increase of the molecular volume (due to the increase of the internal void volume,  $V_{\text{M}}^{\text{empty}}$ ), and by the expansion of the protein/solvent interface with temperature.

To illustrate the origin of the pressure dependence of the solvent contribution  $\Delta V$ , we follow eqn (8). In our approach, the hydration shell is represented by Voronoi shells, and it has

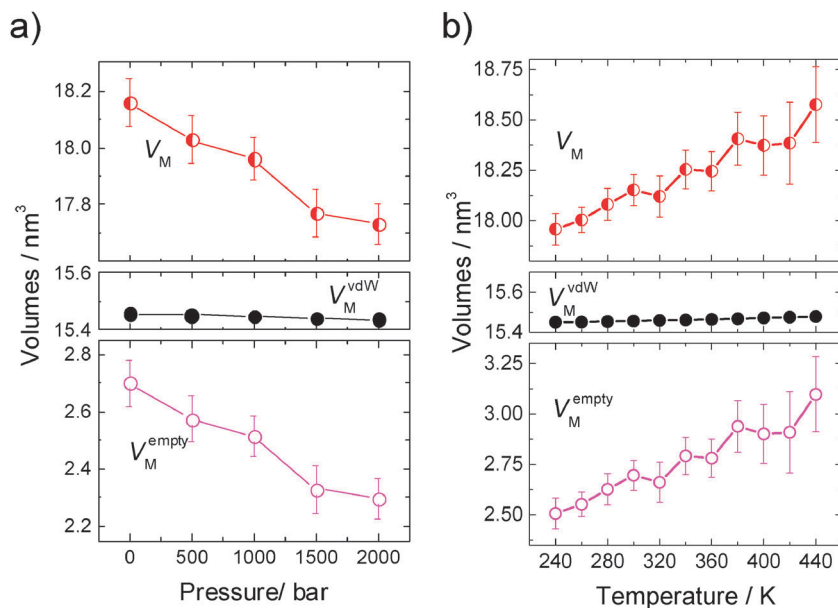


Fig. 4 Components of the molecular volume,  $V_M$  ( $V_M = V_M^{vdW} + V_M^{empty}$ ). (a) Pressure dependence, (b) temperature dependence (adopted from ref. 49). It is clearly seen that the internal voids make up the main contribution to the pressure and temperature dependence of the molecular volume,  $V_M$ .

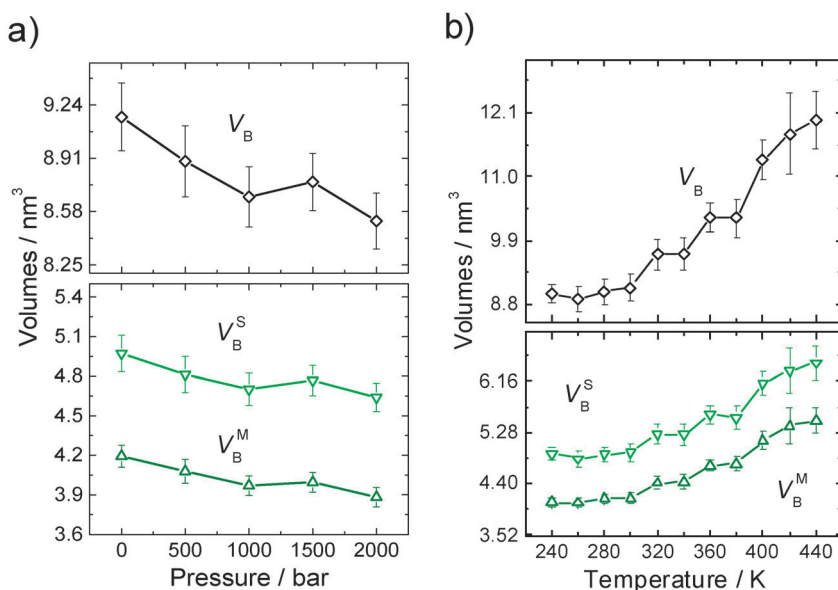


Fig. 5 The boundary volume,  $V_B$ , and its components ( $V_B = V_B^M + V_B^S$ ) of SNase. (a) Pressure dependence, (b) temperature dependence (adopted from ref. 49).

been shown that only the first Voronoi shell experiences significant differences of the water density compared to bulk water.<sup>51</sup> Thus we can write

$$\Delta V \approx V_1 - n_1 v_0, \quad (11)$$

where  $V_1$  is the mean volume of the first Voronoi shell around the protein molecule,  $n_1$  is the mean number of water molecules in the first Voronoi shell, and  $v_0$  is the mean volume of a Voronoi cell for bulk water molecules ( $v_0 = 1/\rho_0$ ). As the size of the water molecule is constant, we can also write:

$$\Delta V \approx \Delta V' = V_1^{empty} - n_1 v_0^{empty}, \quad (12)$$

where  $V_1^{empty}$  is the mean empty volume in the first Voronoi shell (light-green and yellow parts in Fig. 1), and  $v_0^{empty}$  is the corresponding mean empty volume of the Voronoi cell for bulk water. We calculated the values of  $V_1^{empty}$  and  $n_1 v_0^{empty}$  as well as their difference  $\Delta V' = V_1^{empty} - n_1 v_0^{empty}$  for our models of SNase solutions at different pressures and temperatures as shown in Fig. 6. We clearly see that  $\Delta V'$  describes the pressure and temperature dependence of  $\Delta V$ , obtained by eqn (5), very well (see Fig. 2 in this paper and Fig. 3 in ref. 49). A small numerical difference between  $\Delta V'$  and  $\Delta V$  supports our assumption that the first Voronoi shell provides a good approximation for the hydration shell around the polypeptide molecule.

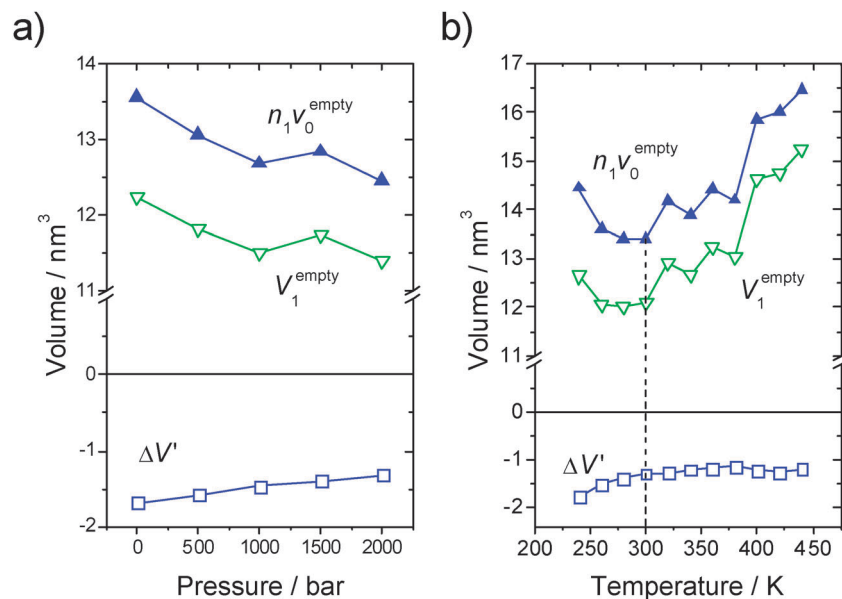


Fig. 6 The mean empty volume of the first Voronoi shell,  $V_1^{\text{empty}}$ , the corresponding volume for bulk water,  $n_1 v_0^{\text{empty}}$ , and their difference  $\Delta V'$  (eqn (12)) for SNase as function of pressures (a) and temperatures (b). The vertical dashed line marks the temperature of  $T = 300$  K, for which the pressure dependent calculations have been carried out.

Hence, the pressure dependence of the solvent contribution  $\Delta V$  to the apparent volume,  $V_{\text{app}}$ , is determined by the pressure dependence of the hydration water's empty space compared to the pressure dependence of the empty space in bulk water. In particular, as we can see in Table 1, the void volume  $V_B^S$  in the hydration shell decreases to a lesser extent than the voids  $V_B^{S,\text{bulk}}$  in a comparable bulk water layer (ref. 51), which is reflected in a two-fold larger contribution of the latter to the (negative) compressibility. As volume is reciprocal to density, we note that the water density in the first Voronoi shell is higher than in bulk water. Hence, the contribution  $\Delta V$  of the solvent is negative. This difference decreases slightly with increasing pressure because the density of the hydration shell increases less than that of bulk water (see Fig. 6a). A similar behavior holds true for the temperature dependence of  $\Delta V$ . The water density in the first Voronoi shell is also higher than in the bulk, rendering  $\Delta V$  negative, and the density difference decreases slightly with increasing temperature. However, in this case, the density of the hydration shell decreases more than that of bulk water (Fig. 6b). Of note, the density changes discussed here are an outcome of averaging over different parts of the protein surface, and in general should be different for charged and non-polar sites. The Voronoi–Delaunay approach introduced here could in fact be used to analyze different sites.<sup>52</sup>

Recall, as demonstrated in ref. 51, that we can write eqn (12) in a different form:

$$\Delta V = V_B^S - f n_1 v_0^{\text{empty}}, \quad (13)$$

where  $f = 0.485$ .<sup>51</sup> The entire Voronoi shell is used in eqn (12) to determine  $\Delta V$ , whereas eqn (13) contains only the inner part of the first Voronoi shell,  $V_B^S$  (see Fig. 1). The subtrahend of eqn (13) is the void volume of a water layer in bulk water that is comparable to the volume  $V_B^S$  and had been called  $V_B^{S,\text{bulk}}$  in

ref. 51. Using eqn (13) and (6), we can rewrite eqn (4) in a simple form:

$$V_{\text{app}} = V_M + V_B - f n_1 v_0^{\text{empty}}, \quad (14)$$

where the total boundary volume,  $V_B$ , is an explicit term of the equation now.

Small kinks observed in the temperature dependent data of  $V_1^{\text{empty}}$  and  $n_1 v_0^{\text{empty}}$  in Fig. 6 are probably due to fluctuations of  $n_1$  values, which are due to slightly different configurations of the protein molecule, possibly reflecting an insufficient averaging over the complete ensemble of configurations at the given state point. What is clear, however, is that their difference (eqn (12)) is a rather smooth function of temperature and pressure. This indicates that the properties of the hydration shell are not very sensitive to conformational changes of the molecule.

### Alternative approaches for dissecting the apparent volume of a protein

There are also alternative approaches possible for partitioning of the apparent volume,  $V_{\text{app}}$ . Above, we used a geometrical approach to select shells related with the solute molecule. In another approach, following Chalikian *et al.*,<sup>21</sup> one might decompose the apparent volume as:

$$V_{\text{app}} = V_M + V_T + V_I, \quad (15)$$

where  $V_T$  is the “thermal volume”, which is the volume of the void space surrounding the solute molecule as a result of thermally induced mutual molecular vibrations and reorientations of the solute and the solvent, and  $V_I$  is the “interaction volume”, which represents the change in the solvent volume under the influence of solute–solvent interactions.<sup>21</sup> It is generally assumed that  $V_I$  predominantly reflects a decrease in the solvent

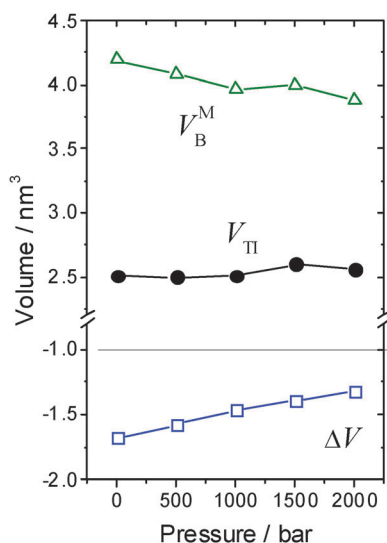


Fig. 7 Pressure dependence of the volume  $V_{Ti}$  and its components  $V_B^M$  and  $\Delta V$  for SNase.

volume that results from hydration of polar and charged solute groups (the so-called electrostriction effect). Please note that the parameters  $V_T$  and  $V_I$  have no direct geometrical interpretation

and are hence difficult to quantify. The volume term  $V_T$  is related to the fact that the “cavity” of the solute molecule created by inserting the molecule into the solvent should be larger than its molecular volume, and this extra volume should be sensitive to temperature.<sup>21</sup>

Denoting the sum of the non-molecular components  $V_T$  and  $V_I$  as  $V_{Ti}$ , we obtain from eqn (15)

$$V_{Ti} = V_{app} - V_M \quad (16)$$

In analogy to eqn (5), one can denote the parameter  $V_{Ti}$  the “contribution of the environment” of the solute. It differs from the above defined “contribution of the solvent”,  $\Delta V$ , by the volume of the boundary voids assigned to the molecule. Using eqn (9) and (7) we can rewrite eqn (16):

$$V_{Ti} = V_B^M + \Delta V \quad (17)$$

Thus, the value of  $V_{Ti}$  can be represented by our volumetric parameters, which can be calculated from molecular dynamics models. Fig. 7 depicts the components of eqn (17).

We notice that  $V_{Ti}$  is positive and rather insensitive to pressure. Its components change with pressure but they exhibit an opposite behavior: the boundary volume,  $V_B^M$ , of the molecule decreases, whereas the solvent contribution,  $\Delta V$ ,

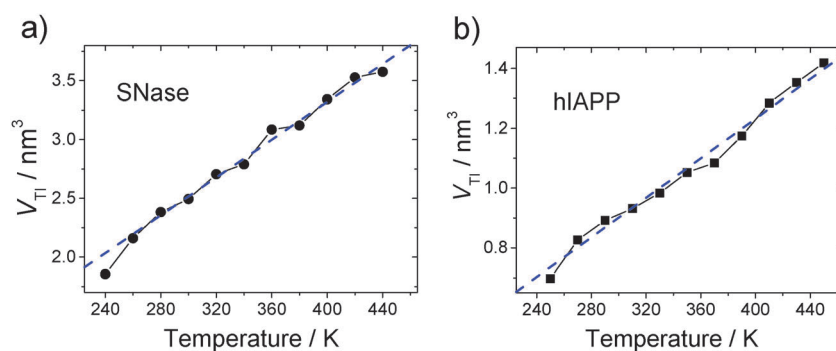


Fig. 8 Temperature dependence of the parameter  $V_{Ti} = V_B^M + \Delta V$  for SNase (a) and hIAPP (b) at ambient pressure. Dashed lines are linear extrapolations of the calculated curves.

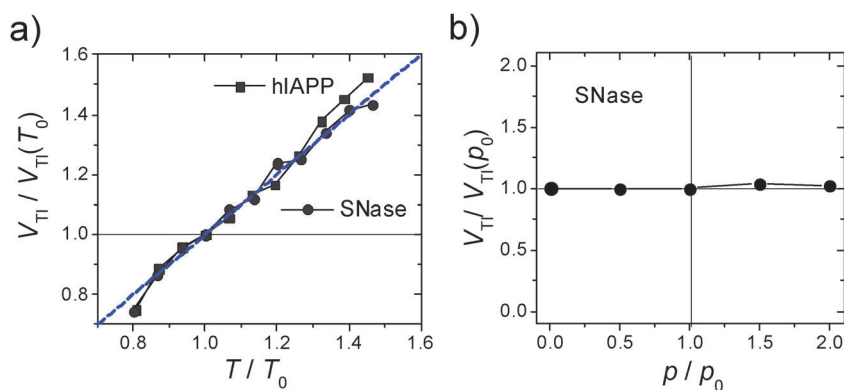


Fig. 9 Temperature dependence of  $V_{Ti} = V_B^M + \Delta V$  for SNase and hIAPP represented in normalized coordinates,  $T/T_0$  and  $V_{Ti}/V_{Ti}(T_0)$ , where  $T_0 = 300$  K. The dashed line is a bisector of the coordinate system (a). Pressure dependence of  $V_{Ti} = V_B^M + \Delta V$  represented in normalized coordinates,  $p/p_0$  and  $V_{Ti}/V_{Ti}(p_0)$ , where  $p_0 = 1000$  bar (b).

increases upon compression. As the interaction volume  $V_I$  (via electrostatic and dipole–dipole protein–solute interactions) is not expected to change the density of water around the protein significantly in the pressure range covered here, the pressure dependence of the thermal volume  $V_T$  will be small as well.

To reveal also the temperature dependence of  $V_{TI}$ , we calculated this parameter for our MD models of SNase and hIAPP at different temperatures. As shown in Fig. 8,  $V_{TI}$  is linearly temperature dependent for both molecules.

In case the interaction volume  $V_I$  is independent of temperature, the  $V_{TI}$  data shown in Fig. 8 would imply a pronounced and linear temperature dependence of the thermal volume,  $V_T$ . Interestingly, the temperature dependence of  $V_{TI}$  seems to be universal for both peptides. This is better seen in Fig. 9a, which depicts the temperature dependence of  $V_{TI}$  when normalized to room temperature conditions ( $T = 300$  K). In contrast, the normalized pressure dependent data (Fig. 9b) reveal that  $V_{TI}$  is essentially independent of pressure.

## Conclusions

We used the decomposition of a molecular dynamics model of SNase in its natively folded state in aqueous solution into Voronoi and Delaunay shells to analyze the pressure dependence of the apparent volume of the protein,  $V_{app}$ , and its contributing components: the Voronoi volume of the solute molecule,  $V_{Vor}$ , which is considered as the intrinsic volume, the molecular volume,  $V_M$ , which consists of the van der Waals volume,  $V_M^{vdw}$ , and its internal empty voids,  $V_M^{empty}$ , and the contribution of the solvent,  $\Delta V$ , with respect to bulk water. Additionally, we geometrically separated the boundary volume  $V_B$  at the solute/solvent interface into two parts, which are assigned to the macromolecule,  $V_B^M$ , and the solvent,  $V_B^S$ . The coefficient of the isothermal compressibility of  $V_{app}$ ,  $\beta_{T,app}$ , and its components have also been calculated. The calculated value of  $\beta_{T,app}$  is in good agreement with the experimental data obtained by densitometric measurements.<sup>15</sup> The pressure dependences are compared with the temperature dependences, obtained in our previous study.<sup>49</sup>

The Voronoi volume of the molecule consists of the molecular volume and of a part of boundary voids assigned to the solute,  $V_{Vor} = V_M + V_B^M$ . It defines the “cavity” in the solvent where the protein has been placed. Our results show a strong decrease of both components of the Voronoi volume with pressure: (i) of the molecular volume,  $V_M$ , owing to a pronounced decrease of its internal void volume,  $V_M^{empty}$ , upon compression, with isothermal compressibility values of  $\sim 0.95 \times 10^{-5} \text{ bar}^{-1}$ , and (ii) of the boundary voids belonging to the molecule, with compressibility values of  $\sim 0.83 \times 10^{-5} \text{ bar}^{-1}$ . The pressure dependence of the Voronoi volume,  $V_{Vor}$ , is opposite to the temperature dependence.  $V_{Vor}$  increases with temperature, mainly because of a strong and universal increase of the boundary volume  $V_B^M$  of the solute with temperature.

The behavior of the contribution of the solvent,  $\Delta V$ , upon changes of temperature and pressure is a result of the competition between changes of the density of water in the hydration shell of the solute and that of bulk water. At ambient conditions, the value of  $\Delta V$  for SNase is negative, indicating that the hydration water is denser than bulk water. With increasing pressure, the void volume in the hydration shell decreases to a lesser extent than the voids in bulk water. Conversely, with increasing temperature the void volume of the hydration shell increases more than that of bulk water. The different temperature and pressure dependent behavior of the hydration and bulk water produces, however, similar results for their  $\Delta V$  dependences.

We conclude that the decrease of  $V_{app}$  of SNase with pressure is essentially due to the compression of the molecular volume. Thus, the remainder of the apparent and the molecular volumes,  $V_{app} - V_M$ , is practically insensitive to pressure. On the other hand, we found that it increases linearly with temperature. Of note, this remainder is equal to the sum of  $V_T + V_I$ , where  $V_T$  is the “thermal volume” and  $V_I$  the solvent “interaction volume” as defined by Chalikian *et al.*<sup>21</sup>

A closer inspection of Fig. 3 to 5 reveals a more pronounced decrease of the empty void volume,  $V_M^{empty}$ , and a retarded decrease of the boundary volume,  $V_B^M$ , around 1500 bar. This points to a minor expansion of the SNase molecule due to pressure-induced conformational fluctuations in this pressure range, leading to an increase of the interfacial region and its void volume. In fact, this is the pressure range, where the onset of the pressure-induced unfolding of SNase has been recorded experimentally.<sup>13</sup> Verification of these assumptions requires further investigations, however.

Finally, we hope that our results help to understand and decompose the volumetric properties of biomolecular systems, including their pressure dependence. Our results show that the volumetric properties of proteins are strongly coupled to changes of the hydrational properties at their interface with respect to the bulk properties of the solvent, as well as to the compressibility of the internal voids of the protein. Using this Voronoi–Delaunay approach might enable us to unravel the various volumetric contributions of even more complex biologically relevant systems and processes in future studies, including, for example, enzymatic reactions carried out under high pressure conditions (baroenzymology).

## Acknowledgements

Financial support from Alexander von Humboldt Foundation, grants from RFFI (No. 15-03-03329) and the DFG (FOR 1979 and the Cluster of Excellence RESOLV (EXC 1069)) are gratefully acknowledged.

## References

- 1 P. L. Privalov and S. J. Gill, *Adv. Protein Chem.*, 1988, **39**, 191–234.



- 2 K. A. Dill, *Biochemistry*, 1990, **29**, 7133–7155.
- 3 Y. Levy and J. N. Onuchic, *Annu. Rev. Biophys. Biomol. Struct.*, 2006, **35**, 389–415.
- 4 P. W. Bridgman, *J. Biol. Chem.*, 1914, **19**, 511–512.
- 5 C. A. Royer, *Biochim. Biophys. Acta, Protein Struct. Mol. Enzymol.*, 2002, **1595**, 201–209.
- 6 J. F. Brandts, R. J. Oliveira and C. Westort, *Biochemistry*, 1970, **9**, 1038–1047.
- 7 S. A. Hawley, *Biochemistry*, 1971, **10**, 2436–2442.
- 8 A. Zipp and W. Kauzmann, *Biochemistry*, 1973, **12**, 4217–4228.
- 9 G. Weber and H. G. Drickamer, *Q. Rev. Biophys.*, 1983, **16**, 89–112.
- 10 H. Herberhold and R. Winter, *Biochemistry*, 2002, **41**, 2396–2401.
- 11 M. W. Lassalle, H. Yamada and K. Akasaka, *J. Mol. Biol.*, 2000, **298**, 293–302.
- 12 F. Meersman, L. Smeller and K. Heremans, *Biochim. Biophys. Acta, Proteins Proteomics*, 2006, **1764**, 346–354.
- 13 G. Panick, G. J. Vidugiris, R. Malessa, G. Rapp, R. Winter and C. A. Royer, *Biochemistry*, 1999, **38**, 4157–4164.
- 14 J. Wiedersich, S. Kohler, A. Skerra and J. Friedrich, *Proc. Natl. Acad. Sci. U. S. A.*, 2008, **105**, 5756–5761.
- 15 H. Seemann, R. Winter and C. A. Royer, *J. Mol. Biol.*, 2001, **307**, 1091–1102.
- 16 K. Akasaka, *Chem. Rev.*, 2006, **106**, 1814–1835.
- 17 J. L. Silva, D. Foguel and C. A. Royer, *Trends Biochem. Sci.*, 2001, **26**, 612–618.
- 18 R. Winter, D. Lopes, S. Grudzielanek and K. Vogtt, *J. Non-Equilib. Thermodyn.*, 2007, **32**, 41–97.
- 19 R. Mishra and R. Winter, *Angew. Chem., Int. Ed.*, 2008, **47**, 6518–6521.
- 20 S. Suladze, M. Kahse, N. Erwin, D. Tomazic and R. Winter, *Methods*, DOI: 10.1016/j.ymeth.2014.08.007.
- 21 T. V. Chalikian, *Annu. Rev. Biophys. Biomol. Struct.*, 2003, **32**, 207–235.
- 22 T. V. Chalikian, M. M. Totrov, R. A. Abagyan and K. J. Breslauer, *J. Mol. Biol.*, 1996, **260**, 588–603.
- 23 L. Mitra, J. B. Rouget, B. Garcia-Moreno, C. A. Royer and R. Winter, *ChemPhysChem*, 2008, **9**, 2715–2721.
- 24 L. Mitra, N. Smolin, R. Ravindra, C. Royer and R. Winter, *Phys. Chem. Chem. Phys.*, 2006, **8**, 1249–1265.
- 25 K. L. Schweiker, V. W. Fitz and G. I. Makhatadze, *Biochemistry*, 2009, **48**, 10846–10851.
- 26 Y. Zhai, L. Okoro, A. Cooper and R. Winter, *Biophys. Chem.*, 2011, **156**, 13–23.
- 27 J. Roche, M. Dellarole, J. A. Caro, D. R. Norberto, A. E. Garcia, B. Garcia-Moreno, C. Roumestand and C. A. Royer, *J. Am. Chem. Soc.*, 2013, **135**, 14610–14618.
- 28 B. Hess, C. Kutzner, D. van der Spoel and E. Lindahl, *J. Chem. Theory Comput.*, 2008, **4**, 435–447.
- 29 S. Pronk, S. Pall, R. Schulz, P. Larsson, P. Bjelkmar, R. Apostolov, M. R. Shirts, J. C. Smith, P. M. Kasson, D. van der Spoel, B. Hess and E. Lindahl, *Bioinformatics*, 2013, **29**, 845–854.
- 30 W. L. Jorgensen, D. S. Maxwell and J. Tirado-Rives, *J. Am. Chem. Soc.*, 1996, **118**, 11225–11236.
- 31 H. J. C. Berendsen, J. R. Grigera and T. P. Straatsma, *J. Phys. Chem.*, 1987, **91**, 6269–6271.
- 32 T. Darden, D. York and L. Pedersen, *J. Chem. Phys.*, 1993, **98**, 10089–10092.
- 33 U. Essmann, L. Perera, M. L. Berkowitz, T. Darden, H. Lee and L. G. Pedersen, *J. Chem. Phys.*, 1995, **103**, 8577–8593.
- 34 W. G. Hoover, *Phys. Rev. A: At., Mol., Opt. Phys.*, 1985, **31**, 1695–1697.
- 35 S. Nose, *Mol. Phys.*, 1984, **52**, 255–268.
- 36 S. Nose and M. L. Klein, *Mol. Phys.*, 1983, **50**, 1055–1076.
- 37 M. Parrinello and A. Rahman, *J. Appl. Phys.*, 1981, **52**, 7182–7190.
- 38 E. E. David and C. W. David, *J. Chem. Phys.*, 1983, **76**, 4611–4614.
- 39 F. M. Richards, *Methods Enzymol.*, 1985, **115**, 440–464.
- 40 P. Procacci and R. A. Scateni, *Int. J. Quantum Chem.*, 1992, **42**, 1515–1528.
- 41 J. Liang, H. Edelsbrunner, P. Fu, P. Sudhakar and S. Subramaniam, *Proteins: Struct., Funct., Genet.*, 1998, **33**, 18–29.
- 42 M. G. Alinchenko, A. V. Anikeenko, N. N. Medvedev, V. P. Voloshin, M. Mezei and P. Jedlovsky, *J. Phys. Chem. B*, 2004, **108**, 19056–19067.
- 43 B. Bouvier, R. Grünberg, M. Nilges and F. Cazals, *Proteins: Struct., Funct., Bioinf.*, 2008, **76**, 677–692.
- 44 G. Neumayr, T. Rudas and O. Steinhauser, *J. Chem. Phys.*, 2010, **133**, 084108.
- 45 A. Okabe, B. Boots, K. Sugihara and S. N. Chiu, *Spatial, Tessellations – Concepts and Applications of Voronoi Diagrams*, John Wiley & Sons, New York, 2000.
- 46 N. N. Medvedev, *Voronoi–Delaunay Method for Non-Crystalline Structures*, SB Russian Academy of Science (in Russian), Novosibirsk, 2000.
- 47 F. Aurenhammer, R. Klein and D. T. Lee, *Voronoi Diagrams and Delaunay Triangulations*, World Scientific Publishing Company, Singapore, 2013.
- 48 V. P. Voloshin, N. N. Medvedev, M. N. Andrews, R. R. Burri, R. Winter and A. Geiger, *J. Phys. Chem. B*, 2011, **115**, 14217–14228.
- 49 V. P. Voloshin, N. N. Medvedev, N. Smolin, A. Geiger and R. Winter, *J. Phys. Chem. B*, 2015, **119**, 1881–1890.
- 50 V. Kim, V. P. Voloshin, N. N. Medvedev and A. Geiger, in *Transactions on Computational Science XX*, ed. M. L. Gavrilova, C. J. K. Tan and B. Kalantari, Springer, Berlin Heidelberg, 2013, vol. 8110, pp. 56–71.
- 51 V. P. Voloshin, A. V. Kim, N. N. Medvedev, R. Winter and A. Geiger, *Biophys. Chem.*, 2014, **192**, 1–9.
- 52 V. Kim, N. N. Medvedev and A. Geiger, *J. Mol. Liq.*, 2014, **189**, 74–80.
- 53 N. N. Medvedev, V. P. Voloshin, A. V. Kim, A. V. Anikeenko and A. Geiger, *J. Struct. Chem.*, 2013, **54**, 271–288.
- 54 S. V. Anishchik and N. N. Medvedev, *Phys. Rev. Lett.*, 1995, **75**, 4314–4317.
- 55 B. J. Gellatly and J. L. Finney, *J. Mol. Biol.*, 1982, **161**, 305–322.
- 56 F. Aurenhammer, *SIAM J. Comput.*, 1987, **16**, 78–96.

- 57 V. P. Voloshin, N. N. Medvedev and A. Geiger, in *Transactions on Computational Science XXII*, ed. M. L. Gavrilova, Springer, Berlin Heidelberg, 2014, vol. 8360, pp. 156–172.
- 58 S. Sastry, T. M. Truskett, P. G. Debenedetti, S. Torquato and F. H. Stillinger, *Mol. Phys.*, 1998, **95**, 289–297.
- 59 H. L. Pi, J. L. Aragonés, C. Vega, E. G. Noya, J. L. F. Abascal, M. A. González and C. McBride, *Mol. Phys.*, 2009, **107**, 365–374.
- 60 I. Brovchenko, M. N. Andrews and A. Oleinikova, *Phys. Chem. Chem. Phys.*, 2010, **12**, 4233–4238.
- 61 A. Ben-Naim, *J. Chem. Phys.*, 2008, **128**, 234501.
- 62 N. Patel, D. N. Dubins, R. Pomes and T. V. Chalikian, *J. Phys. Chem. B*, 2011, **115**, 4856–4862.
- 63 M. Marchi, *J. Phys. Chem. B*, 2003, **107**, 6598–6602.
- 64 V. P. Voloshin, A. V. Anikeenko, N. N. Medvedev and A. Geiger, *Proc. of the 8th ISVD*, 2011, pp. 170–176.